Meteorologische Zeitschrift, Vol. **14**, No. 4, 573-582 (August 2005)

Article

An upgraded estimate of the radiative forcing of cryoplane contrails

SUSANNE MARQUART[1], MICHAEL PONATER*, LINDA STRÖM[2] and KLAUS GIERENS

DLR-Institut für Physik der Atmosphäre, Oberpfaffenhofen, Germany
[1]Present affiliation: Institut für Umweltphysik, Universität Heidelberg
[2]Present affiliation: Volvo Aero Corporation, Trollhättan, Sweden

(Manuscript received January 13, 2004; in revised form September 20, 2004; accepted October 8, 2004)

Abstract

The radiative forcing of contrails is quantified for a hypothetical fleet of cryoplanes in comparison with a conventional aircraft fleet. The differences in bulk optical properties between conventional and cryoplane contrails are determined by numerical simulations of the microphysical evolution of conventional and cryoplane contrails, under several ambient conditions. Both types of contrails contain about the same ice mass, but the mean effective particle radius is found to be smaller by about a factor of 0.3 in conventional contrails than in cryoplane ones. Hence, in case of cryoplanes the contrail optical depth is lower, which counteracts (with respect to radiative forcing) the effect of increased contrail cover due to the higher specific emission of water vapour. If the information gained from the microphysical simulations is translated to the framework of a global climate model, the global mean radiative forcing of cryoplane contrails is simulated to be between about 30% lower and 30% higher compared to the radiative forcing of conventional contrails, depending on the quantitative assumptions made for the mean particle properties and also depending on the time slice considered. Our results indicate that the effect of decreased optical depth is about the same magnitude as the effect of increased contrail cover. Current state of knowledge does not allow a conclusive assessment whether the net radiative impact of cryoplane contrails will be smaller or larger than that of conventional contrails. Uncertainty with respect to radiative forcing arises mainly from insufficient knowledge regarding the mean effective ice crystal radius for both conventional and, especially, cryoplane contrails.

Zusammenfassung

Der Strahlungsantrieb von Kondensstreifen auf Grund einer hypothetisch angenommenen Flotte wasserstoffgetriebener Flugzeuge ("Cryoplanes") wird mit dem entsprechenden Effekt einer herkömmlichen Luftverkehrsflotte verglichen. Die Bestimmung des Unterschiedes der mittleren optischen Eigenschaften für die beiden Typen von Kondensstreifen geschieht durch numerische Simulationen der mikrophysikalischen Entwicklung unter verschiedenen Umgebungsbedingungen. Für beide Arten von Kondensstreifen stimmt die Masse des gebildeten Wolkeneises nahezu überein, aber der mittlere Partikelradius ist für Teilchen in herkömmlichen Kondensstreifen um etwa einen Faktor 0,3 kleiner. Somit ist die optische Dicke von Kondensstreifen aus Cryoplanes geringer; dieser Effekt wirkt – im Hinblick auf die Größe des Strahlungsantriebes – dem Effekt eines sich vergrößernden Bedeckungsgrades durch den höheren spezifischen Emissionsindex von Wasserdampf entgegen. Wird die aus den mikrophysikalischen Simulationen gewonnene Information in ein globales Klimamodell übertragen, so verringert oder erhöht sich der Strahlungsantrieb für die Kondensstreifen aus Cryoplanes gegenüber dem konventionellen Fall um etwa 30 %, je nachdem welche Annahmen für die Partikelgröße und -gestalt im Referenzfall und für die Zeitebene der Betrachtung gemacht werden. Die Ergebnisse deuten darauf hin, dass der Effekt der sich verringernden optischen Dicke und der Effekt des sich erhöhenden Bedeckungsgrades der Kondensstreifen im Cryoplane-Fall etwa gleich stark sind. Der gegenwärtige Wissensstand erlaubt kein abschließendes Urteil, ob die Strahlungswirkung von Cryoplane-Kondensstreifen kleiner oder größer sein würde als diejenige konventioneller Kondensstreifen. Die verbleibenden Unsicherheiten in der Abschätzung der Strahlungsantriebe sind vor allem auf eine mangelhafte Kenntnis des absoluten mittleren Partikelradius in den beiden verglichenen Fällen zurückzuführen.

1 Introduction

Aircraft emissions presently contribute by about 3% to the total radiative forcing from anthropogenic emissions (IPCC, 1999). Since, in the foreseeable future, aviation is likely to be one of the fastest growing economic sectors, it is strongly desirable to reduce its environmental impact. This could be achieved, for instance, by improving aircraft and engine technology resulting in lower specific emissions, or by regulating flight altitudes to ecological flight levels, where the radiative impact of aircraft emissions is minimised. Considering the limited availability of conventional kerosene, the use of alternative fuels such as biomass fuels, liquid natural gas,

*Corresponding author: Michael Ponater, DLR-Institut für Physik der Atmosphäre, Deutsches Zentrum für Luft- und Raumfahrt, Oberpfaffenhofen, 82230 Wessling, Germany, e-mail: michael.ponater@dlr.de

0941-2948/2005/0057 $ 4.50

DOI: 10.1127/0941-2948/2005/0057

and especially liquid hydrogen, has also been discussed (LEWIS and NIEDZWIECKI, 1999). The European research project CRYOPLANE (which lasted from April 2000 to Mai 2002) produced a comprehensive assessment of the technical, economical, and ecological aspects associated with liquid hydrogen powered aircraft (so called cryoplanes) for the first time.

A first estimate of the climate impact of cryoplanes was provided by MARQUART et al. (2001), who compared a fleet of cryoplanes with a conventional, kerosene powered fleet of aircraft, assuming a complete substitution of the conventional fleet by cryoplanes in the year 2015 and a constant air traffic density afterwards. The radiative forcing values of aircraft–induced changes of carbon dioxide, ozone, methane, water vapour, contrails, and aerosol abundance were estimated for both the conventional and the cryoplane scenarios: The radiative impact of all substances except for water vapour and contrails was found to be substantially smaller in the cryoplane case. However, the radiative forcing of contrails was suggested to be large enough to question any environmental superiority of cryoplane operation. Simultaneously, this component was attributed the largest uncertainties, because the specific optical properties of cryoplane contrails were purely speculative at that time. For example, possible differences in ice crystal properties between contrails from cryoplanes and conventional aircraft could not be accounted for by MARQUART et al. (2001).

As there is no cryoplane in flight operation, lack of information about cryoplane contrail properties from measurements is persisting, making it inevitable to rely on numerical model calculations in order to improve knowledge about the specific optical properties of cryoplane contrails. Quite recently, the microphysical evolution of cryoplane contrails was simulated for the first time (STRÖM and GIERENS, 2002). Assuming that, in comparison with "conventional" kerosene powered aircraft, cryoplanes do not emit particles but nearly three times more water vapour, two pairs of simulations were conducted. The results suggested that (under equal ambient conditions) cryoplane contrails contain similar ice masses but significantly less ice crystals than conventional ones, rendering cryoplane contrails optically thinner than their conventional counterparts.

In our present study, we focus on an update of the radiative forcing estimate for cryoplane contrails relying on microphysical information provided by the STRÖM and GIERENS (2002) model. In order to quantify the differences in microphysical and optical properties of cryoplane and conventional contrails for a representative parameter space, we run the numerical model of STRÖM and GIERENS (2002) for quite a number of combinations of ambient temperature and humidity. The resulting information is translated into the framework of a general circulation model (GCM) extended by a specific contrail parameterisation (PONATER et al., 2002) to yield an estimate of the related radiative forcing on the global scale. The contrail parameterisation has already been used for investigating the future development of contrails in case of conventional air traffic (MARQUART et al., 2003).

In the following section, the microphysical simulations and their results are described. The GCM simulations, as well as results for coverage and radiative forcing of cryoplane contrails are presented in section 3, in comparison with conventional contrails. Conclusions are drawn and a short outlook is given in section 4.

2 Microphysical contrail simulations

2.1 Method

Relying on the approach of STRÖM and GIERENS (2002), the microphysical evolution of contrails (up to an age of 30 minutes) is simulated using the MESOSCOP model (SCHUMANN et al., 1987), which has been completed by routines for simulating the thermodynamics of the exhaust and the dynamics of the aircraft wake (SUSSMANN and GIERENS, 2001). The MESOSCOP model has proved its suitability for microphysical contrail simulations in several earlier studies (e.g., GIERENS, 1996; GIERENS and STRÖM, 1998; GIERENS and JENSEN, 1998).

The two spatial dimensions of the model domain are span direction and height. The different phases of contrail formation (jet, vortex, and dispersion phase) are simulated using different resolutions, domains, and time steps. Combustion of kerosene or liquid hydrogen, respectively, is characterised by two sets of initial exhaust specifications: Cryoplanes emit 2.6 times more water vapour per unit of flight path than kerosene powered aircraft, but, in contrast to conventional engines, they do not emit aerosols. Therefore, while ice crystal production in the cryoplane case is modelled by nucleation of the background aerosol, for the conventional case an initial ice crystal distribution can be prescribed, which has been chosen in consistence with in situ measurements (SCHRÖDER et al., 2000). Prognostic variables are water vapour, ice water content, number density of ice crystals, and number densities of two modes of aerosol in the ambient air. More details about the numerical model, the initialisation of the vortex circulation, and the included cloud microphysical processes can be found in STRÖM and GIERENS (2002).

In all microphysical simulations performed for the present paper, we assume a background vertical temperature gradient of –0.65 K/100 m, and a contrail formation at 11 km (247 hPa) altitude. Random fluctuations of vertical and horizontal velocity components (up to

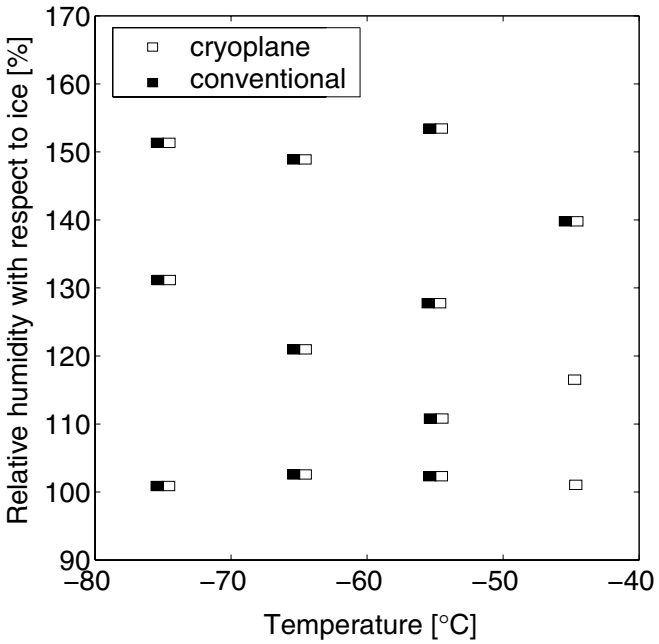

Figure 1: Different combinations of temperature and relative humidity with respect to ice, which were used as input to the microphysical simulations for cryoplanes and conventional aircraft.

±1 m/s) are added to the velocity field for a most simple representation of atmospheric turbulence. For the two aerosol modes, the geometric mean radii, the geometric standard deviations, and the initial particle number densities are prescribed. The distribution of the background aerosol is assumed to be homogeneous, i.e., a possible minimum of particles available for nucleation in the exhaust core is not considered. Such a minimum may form if part of the ambient aerosols slip through the engine bypass while the rest is burned in the combustor. Another potential process, as proposed by CHEN (1999) and discussed by STRÖM and GIERENS (2002), is recondensation of small particles in the exhaust after the larger ambient aerosols have been burned in the combustor; most of these small particles will probably be rather ineffective as condensation nuclei. There are no measurements in a cryoplane wake that would allow to verify the various possibilities. However, the difference in contrail ice crystal density developing in a "homogeneous background" case and in a "zero particle" case appears to be small compared to the uncertainty and variability of the background aerosol density and the ice crystal density produced by kerosene engines, according to sensitivity experiments presented by STRÖM and GIERENS (2002).

We perform 11 pairs of simulations (each consisting of a conventional and a cryoplane case) for various combinations of temperature and relative humidity with respect to ice, scanning the possible range of ambient conditions where contrails may form (Figure 1). For quite high temperatures (–45°C), and moderate relative humidities with respect to ice (<120%), only cryoplane contrails can be simulated since conventional aircraft do not lead to contrail formation at those conditions according to the thermodynamic theory of contrail formation (SCHMIDT, 1941; APPLEMAN, 1953; SCHUMANN, 1996). In most simulations no wind shear is provided, but in order to check the importance of this simplification for the simulated microphysical properties of contrails, we do sensitivity runs for one case of ambient conditions, underlying two different wind profiles (with maximum wind speeds of 2.5 or 5 m/s at 11 km altitude). In contrast to STRÖM and GIERENS (2002), who assessed the temporal evolution of the two kinds of contrails quite thoroughly for their two extreme cases (one "cold" and one "warm" case), we focus (for our 11 pairs of simulations) on a comparison of 30-minute averages, which form a reasonable input for the GCM with its much longer time step.

2.2 Results

The bulk characteristics of the simulated contrails, i.e., total ice crystal number and ice mass per meter of flight path, agree with those reported in STRÖM and GIERENS (2002): The 30-minute average of the ice crystal concentration is about one magnitude lower in cryoplane contrails than in conventional ones under identical ambient conditions. The amount of mean ice mass formed in the contrails is practically the same for both types of fuel, and varies in a consistent way with ambient temperature and relative humidity. Apparently, the water vapour available for condensation in the background atmosphere (ice supersaturation) is the governing parameter for the contrail ice water content (GIERENS, 1996; JENSEN et al., 1998).

The relevant bulk microphysical contrail properties forming the link to the GCM calculations are ice water path, effective ice crystal radius (r_{eff}) and optical properties, the latter being functions of the first two. Hence, the key parameter for the comparison of the contrail climate impact caused by the two aircraft types considered is the effective particle radius. In MESOSCOP, it is calculated for each grid cell depending on the grid cell averaged ice mass per crystal, making certain assumptions about the underlying mass distribution function and the shape of the ice crystals as described by STRÖM and GIERENS (2002). It must be noted that the effective radius for ice crystals (in contrast to liquid droplets) is not very well defined due to the varying shapes possible for crystals (MCFARQUHAR and HEYMSFIELD, 1998; WYSER, 1998; MITCHELL, 2002). Therefore, as was already suggested by STRÖM and GIERENS (2002), we focus our considerations on the ratio between conventional and cryoplane effective particle radii. In this way, the inherent uncertainties in the r_{eff}-definition can be expected to cancel out, at least partially. Furthermore, ratios should

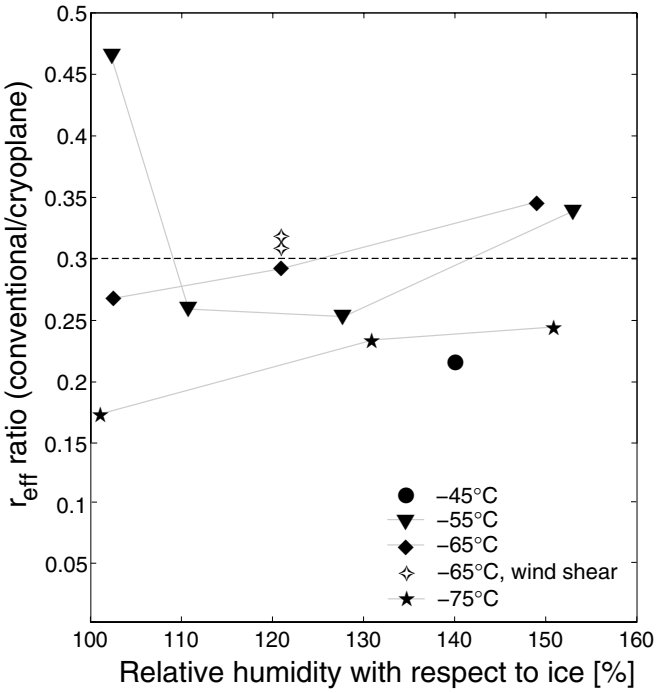

Figure 2: The ratios of the 30-minute averaged, crystal density weighted effective radii (r_{eff}) for conventional/cryoplane contrails. The symbols denote different temperatures. For filled symbols, no wind shear is provided. For hollow symbols, vertical wind shear (i.e., a vertical wind profile with maximum wind speeds of 2.5 or 5 m/s at 11 km altitude) is provided.

be less sensitive to uncertainties in the simulations arising from too simplistic assumptions about background aerosol, turbulence, wind shear, etc.

In the GCM, the effective radius is calculated for each 30-minute time step as an average over the whole contrail-covered part of a model grid box, depending on the actual contrail ice water content (HEYMSFIELD, 1977; MCFARLANE et al., 1992). Since the temporal and spatial resolution of the GCM is necessarily coarse in comparison to the microphysical model, we calculate from the latter averages over the 30 minute simulation time and the respective contrail cross section. There are various possibilities of calculating the spatial mean by, e.g., weighting with ice crystal number concentration, ice mass, or area. We chose the ice crystal number weighted average, since it proved to be most consistent with the GCM's bulk formulation relating mean optical depth to mean ice water path and effective radius.

The ratios of the 30-minute averaged, crystal number weighted effective radii for conventional/cryoplane contrails are shown in Figure 2 for all pairs of numerical simulations. For conventional contrails, the effective ice crystal radius is always significantly smaller than for cryoplane contrails, the ratios being below 0.5 (i.e., varying between 0.17 and 0.46). For both kinds of fuel, the mean effective radius increases with increasing supersaturation and increasing temperature, as expected. The ratios, however, do not exhibit a straightforward systematic depencency on temperature and relative humidity (Figure 2): At large supersaturations, the ratio tends to be larger than at small supersaturations for the temperatures –65°C and –75°C, but this does not hold for the –55°C simulations. In addition, the ratio does not vary systematically with changing temperature. (This shows that the two extreme cases discussed by STRÖM and GIERENS (2002) alone do not provide "representative" information about the differences between cryoplane and conventional aircraft effective radii.) The mean effective ice crystal radius of contrail particles increases with increasing vertical wind shear for both types of contrails, as indicated by our sensitivity experiments (not shown). However, the r_{eff}-ratio is found to be nearly independent of wind shear (Figure 2), supporting the choice of the ratio as a relative measure instead of absolute numbers.

As the variation of the r_{eff}-ratios in the T,RH–parameter space are not as straightforward to suggest a convincing statistical-empirical relationship, we decided to run the GCM calculations by simply assuming a constant value of 0.3 for this ratio, adding two respective sensitivity studies where ratios of 0.25 or 0.35 were used instead. The exact procedure employed will be described in the following section.

3 GCM contrail simulations

3.1 Method

The GCM simulations discussed in this section are based on exactly the same model setup as was used by MARQUART et al. (2003) for various contrail radiative forcing estimates. This allows for a consistent comparison with their results. Our basic GCM is the ECHAM4.L39(DLR) model (ROECKNER et al., 1996; LAND et al., 1999, 2002), which we use in a spectral horizontal T30 resolution with a time step of 30 minutes. The model has 39 layers between the surface and the top layer centered at 10 hPa. The GCM was extended by a contrail parameterisation scheme which is based on the thermodynamic theory of contrail formation (PONATER et al., 2002). Contrails may form at any model time step depending on ambient temperature, relative humidity and natural cloudiness, also considering air traffic density for each grid box. The simulated contrails are characterised by a fractional coverage, an individual ice water path and an effective particle radius, as well as optical properties. In order to account for the nonsphericity of ice particles, the respective asymmetry parameter is reduced by an empirical factor of 0.91 in the radiative transfer calculations (ROECKNER, 1995; PONATER et al., 2002). Use is made of an improved way to represent cloud overlap in the ECHAM4 longwave radiation scheme (RÄISÄNEN, 1998; MARQUART

and MAYER, 2002), as has been done in MARQUART et al. (2003). The radiative forcing of contrails is determined as the difference of radiative fluxes with and without contrails. As a measure of climate change we use the stratosphere adjusted radiative forcing at the tropopause (e.g., HANSEN et al., 1997), which is calculated online in the ECHAM4 model (STUBER et al., 2001).

We have performed time slice simulations (i.e., the annual cycles of boundary conditions are held fixed) for the years 2015 and 2050, assuming fleets of aircraft consisting either exclusively of conventional aircraft or of cryoplanes, respectively. The latter are characterised by a higher emission index of water vapour (for absolute values see MARQUART et al., 2001). As a measure of air traffic movements, we use 3D inventories of fuel consumption for 2015 (DLR inventories, SCHMITT and BRUNNER, 1997) and 2050 (NASA inventories, scenario FESGa, BAUGHCUM et al., 1998; CAEP/4-FESG, 1998). Concerning the overall efficiencies of propulsion, we anticipate an increase from 0.3 in 1992 to 0.4 in 2015 and to 0.5 in 2050 (GIERENS et al., 1999; MARQUART et al., 2003). Current state of knowledge suggests that propulsion can be made equally efficient for both kinds of engines (e.g., CORCHERO and MONTANES, 2003; SVENSSON et al., 2004). Possible future changes in the background climate are neglected for simplicity, because climate change can be expected to affect conventional and cryoplane contrails in the same qualitative way. As reference cases for the conventional fleet in 2015 and 2050, we choose those simulations reported in MARQUART et al. (2003), in which climate change is neglected but improvements of overall propulsion efficiency are taken into account. For more insight into the effects of a changing climate and of changing propulsion efficiencies on contrails see MARQUART et al. (2003).

Contrail optical properties are calculated in the GCM contrail parameterisation as functions of the two variables ice water path and effective ice crystal radius within the contrail covered part of a grid box (ROECKNER et al., 1996; PONATER et al., 2002). The mean effective ice crystal radius is calculated from the ice water content using an empirical function (HEYMSFIELD, 1977; MCFARLANE et al., 1992). This bulk formulation yields values ranging from about 12 to 15 μm for contrails in the reference study for the conventional case, which agrees reasonably well with respective observations (see PONATER et al., 2002, and MARQUART et al., 2003, for details). According to the results of the microphysical simulations (section 2), the contrail ice water path can be taken as simulated by the GCM, i.e., independent of the type of aircraft engine, while the ratio between the 30-minute averaged effective radii of conventional/cryoplane contrail particles should be about 0.3. The latter information is fed into the GCM framework by setting up a cryoplane reference case which differs from the conventional reference case only by a larger effective ice crystal radius to any time step:

$$r_{\mathrm{eff}}^{\mathrm{cryo}}(t) = r_{\mathrm{eff}}(t)/0.3 \qquad (3.1)$$

Beyond this standard case we also perform sensitivity studies using ratios of 0.25 and 0.35 in order to account for the uncertainty of this value. Due to the modification of the effective radius in cryoplane contrails, the optical properties, e.g., the contrail optical depth, change accordingly.

Since the contrail net radiative forcing depends nonlinearily on the effective radius (MARQUART et al., 2003; their Fig. 9), and since the knowledge about a "real" typical mean effective radius is poor, we have performed a pair of sensitivity experiments (for the time slice 2015 only) with half the effective particle sizes compared to the respective reference cases. In addition, we have performed a sensitivity simulation for spherical ice particles (by switching off the empirical correction factor for the asymmetry parameter, see above), in order to account for the uncertainty in contrail particle shape.

3.2 Results

Due to the higher specific emission of water vapour in the exhaust gas, the contrail formation frequency would be higher for a fleet of cryoplanes than for an equivalent fleet of kerosene powered aircraft. This is reflected by an increase in total (i.e., vertically integrated) contrail cover in the former case (see MARQUART et al., 2001). If conventional aircraft are completely replaced by cryoplanes, total coverage increases strongest in heavy air traffic regions (USA, Europe, Southeast Asia; Figure 3a), whereas the largest relative increase occurs in the tropics (Figure 3c). However, contrails are only visible (from satellite or an Earth-bound observer) if their optical depth exceeds a certain threshold value. In our studies, we have used a visibility-threshold of 0.02 and, therefore, have distinguished between the "visible" contrail cover and the cover with "all" contrails (PONATER et al., 2002; MARQUART et al., 2003). Though, as just explained, the coverage with all contrails increases all over the world in the our cryoplane simulations (Figure 3a, c), the coverage with visible contrails decreases over a substantial part of the globe (Figure 3b, d): Due to the larger mean effective ice crystal size in combination with an almost unchanged ice water path, cryoplane contrails are characterised by less, but larger ice crystals in comparison with conventional contrails. Therefore, the optical depth of cryoplane contrails is lower, rendering a larger relative part of contrails "invisible". The relative decrease in visible contrail cover is strongest in low-temperature regions, where the optical depth is generally

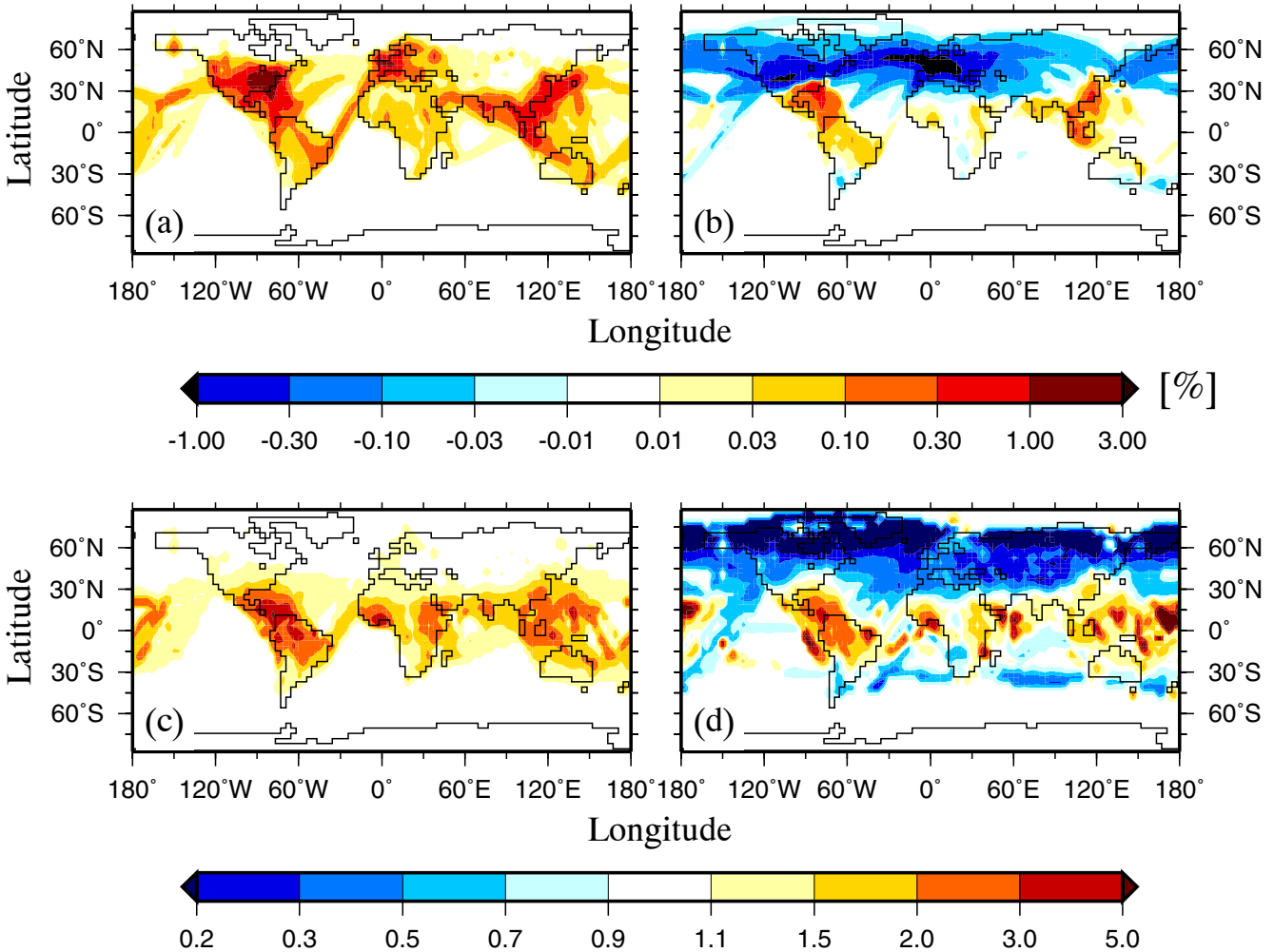

Figure 3: Change in annual mean total contrail cover for the time slice 2015 if the conventional fleet of aircraft is replaced by a fleet of cryoplanes. (a) difference cryoplane-conventional for all contrails; (b) difference cryoplane-conventional for visible contrails; (c) ratio cryoplane/conventional for all contrails; (d) ratio cryoplane/conventional for visible contrails.

Table 1: Global annual mean total contrail cover for conventional and cryoplane air traffic in 2015 and 2050.

Year	Conventional contrail cover [%] visible contrails	all contrails	Cryoplane contrail cover [%] visible contrails	all contrails
2015	0.15	0.23	0.10	0.30
2050	0.28	0.45	0.18	0.54

low (see PONATER et al., 2002), i.e., at high northern latitudes (Figure 3d).

In the global annual mean, the coverage with all contrails would increase by about a factor of 1.3 from 0.23% to 0.30%, if conventional aviation were replaced by cryoplane air traffic in a 2015 scenario (Table 1). The respective visible contrail cover would decrease by a factor of 1.5 from 0.15% to 0.10%. In 2050, the substitution of conventional aviation by a fleet of cryoplanes would leed to a slightly weaker increase in the coverage with all contrails (by a factor of 1.2 only). This is a result of the higher aircraft overall propulsion efficiency in 2050, which facilitates the formation of contrails in a qualitatively similar way as the increase in the specific water vapour emissions (SCHUMANN, 2000; his eq. 14).

As cryoplane contrails may form at a higher ambient temperatures than those from kerosene–driven aircraft (SCHUMANN, 1996), the relative increase in coverage for all contrails is strongest in those regions, where the temperature is close to the thermodynamic threshold for contrail formation in the conventional case: The relative increase is stronger in tropical than in extratropical latitudes (Figure 3c), it is stronger at low altitudes (well below 200 hPa) than at high altitudes (compare also MARQUART et al., 2001; their Fig. 6), and it is stronger in summer than in winter. Due to this latter effect, the pro-

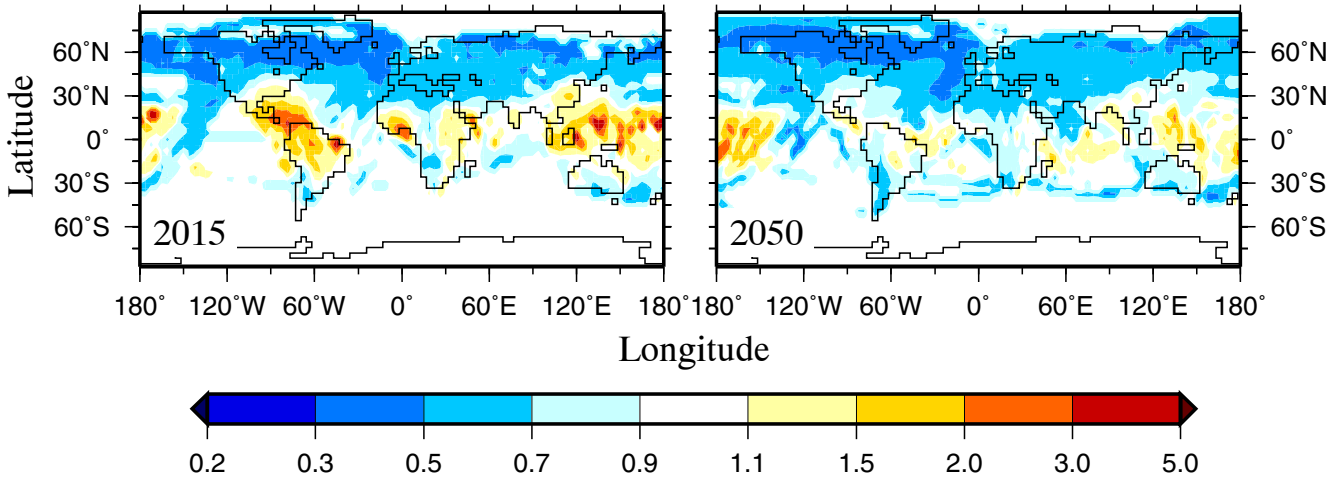

Figure 4: Ratio of annual mean net radiative forcing between cryoplane and conventional contrails for the time slices 2015 (left) and 2050 (right).

nounced global minimum in total contrail cover during the northern hemisphere summer found by PONATER et al. (2002; their Table 1) for the conventional fleet of aircraft is much less pronounced in the cryoplane case (not shown).

At high temperatures (near the thermodynamic threshold), where the relative increase in contrail cover is strongest for the cryoplane scenarios, contrail optical depth is normally larger than at low temperatures due to the larger amount of ambient water vapour available for condensation (PONATER et al., 2002). Hence, there is a tendency towards a preference of relatively large ice water content values if one switches from the conventional to the cryoplane case. Consequently, if we neglect for the moment systematic differences in particle size and consider only differences in contrail cover, we find that global mean radiative forcing would increase even stronger than contrail cover: Radiative forcing would grow by a factor of about 1.7 in 2015 (from 9.8 mW/m^2 to 16.5 mW/m^2), whereas contrail cover would grow by a factor of 1.3 only (Table 1).

If the differences in effective ice crystal size for the different kinds of contrails are taken into account, radiative forcing does not necessarily increase for the cryoplane air traffic since the effect of increasing contrail cover (of all contrails) counteracts the effect of decreasing optical depth. The net effect on the geographical distribution is shown in Figure 4 as the ratio of net radiative forcing between cryoplane and conventional contrails: While in a large part of the tropics the effect of contrail cover exceeds the effect of a lower mean optical depth on radiative forcing (i.e., radiative forcing increases), it is just the other way round in the mid and high latitudes (i.e., radiative forcing decreases). In 2050, the relative decrease in radiative forcing for the cryoplane case is more pronounced than in 2015 due to the relatively smaller increase in contrail cover (see above). In the global and annual mean, radiative forcing decreases from 9.8 mW m^{-2} for the conventional reference case to 8.0 mW m^{-2} for the cryoplane reference case in 2015 (or 19.5 to 13.9 mW m^{-2} for 2050, respectively), suggesting a lower climate impact due to contrails from a fleet of cryoplanes than from an equivalent fleet of kerosene–powered aircraft. If we use r_{eff}-ratios of 0.25 or 0.35 in otherwise identical simulations, the global radiative forcing for the 2015 cryoplane case either decreases to 7.4 mW m^{-2} or increases to 8.9 mW m^{-2}, respectively, which is both still lower than the respective value for the conventional fleet. We may also recall here that the values for global mean contrail radiative forcing reached by means of the GCM parameterisation are generally about a factor of 5 lower than the best estimate provided in IPCC (1999). A detailed discussion of this finding has been given in MARQUART et al. (2003).

Up to now, we have relied on the GCM simulated effective ice crystal radius for conventional aviation, which agrees with that derived from modelled size distributions (STRAUSS et al., 1997) and particle sizes assumed in different model studies (MEERKÖTTER et al., 1999; MINNIS et al., 1999). However, the time-step averaged effective radius for contrail ice particles as used in our simulations is a crucial parameter involving considerable uncertainty since (1) a "typical" effective radius is difficult to define from in situ–observations and (2) neglecting the underlying particle size distribution may lead to systematic errors in the respective radiative forcing calculations (see discussion in MARQUART et al., 2003). Therefore, we have performed a pair of sensitivity studies assuming half the effective particle sizes as calculated by the GCM (which forms an extreme case, quite on the low end of available observations for the conventional air traffic). In this case, the global annual mean net radiative forcing (in 2015) shows quite a different behaviour as it increases from 10.2 mW m^{-2} for

Table 2: Global annual mean net radiative forcing for different realisations of conventional and cryoplane air traffic scenarios in 2015 and 2050. The original values calculated from the ECHAM4 radiation scheme are found in brackets. The main values, which are adjusted by a 25% offset to the longwave global mean contrail radiative forcing (see MARQUART and MAYER, 2002; MARQUART et al., 2003), are disscussed in the text as the best estimate.

Year	Particle Properties	Net Radiative Forcing [mW m^{-2}] Conventional	Cryoplane
2015	non-spherical	9.8 (6.4)	8.0 (5.5)
2015	non-spherical, half size	10.2 (5.6)	13.0 (8.7)
2015	spherical, half size	12.7 (8.2)	
2050	non-spherical	19.5 (12.8)	13.9 (9.5)

the conventional case to 13.0 mW m^{-2} for the cryoplane case (Table 2). Another sensitive fact to be considered here is that small ice particles are more likely to be of nearly spherical shape (SCHRÖDER et al., 2000). Hence, if we assume the quite small ice particles in the conventional case of this sensitivity experiment to be of spherical shape, we end up with a global radiative forcing of 12.7 mW m^{-2}, which comes very close to the 13.0 mW m^{-2} for the cryoplane case.

4 Conclusions and outlook

In order to extend the basis for quantifying the global climate impact of a hypothetical fleet of cryoplanes in comparison with a conventional fleet of aircraft, simulations were performed with the microphysical model MESOSCOP (STRÖM and GIERENS, 2002) and with the ECHAM4 global climate model, which may be run with a specific contrail parameterisation (PONATER et al., 2002). The differences in bulk microphysical properties between conventional and cryoplane contrails were determined by numerical simulations of the microphysical evolution of conventional and cryoplane contrails, respectively. As an outcome of these simulations, both types of contrails contain about the same ice mass, but differ with respect to the mean particle size: The 30-minute averaged, number concentration weighted effective ice crystal radius is about a factor of 0.3 smaller for conventional contrails than for cryoplane contrails.

If this information about the qualitative differences in microphysical contrail properties is translated to the GCM framework, the global mean radiative forcing of cryoplane contrails is simulated to be by about 20% lower in 2015 (or 30% in 2050) compared to the radiative forcing of conventional contrails. The global mean decrease in radiative forcing results from the decrease in contrail optical depth, which outweighs the effect of increased contrail cover due to the higher specific emission of water vapour. However, in tropical regions, where it is often too warm for contrail formation in the case of conventional aircraft, the increase in contrail cover for the cryoplane case is found to be relatively strong, leading to an increase in radiative forcing there. Unfortunately, the uncertainties regarding the mean effective particle sizes even within conventional contrails are quite large, rendering our GCM simulation results more uncertain, too. For instance, our sensitivity studies assuming different absolute particle sizes and shapes indicate that a conclusive answer to the question whether the globally averaged radiative forcing of cryoplane contrails is smaller than that of conventional contrails or not, is not possible with the current state of knowledge. For a validation of the microphysical contrail properties, it would be strongly desirable to compare model results to observations, i.e., measurements taken in the wake of a prototype cryoplane, which presently do not exist.

Nevertheless, our studies suggest a considerably lower climate impact due to cryoplane contrails than estimated by MARQUART et al. (2001): First, the effect of the smaller optical depth of cryoplane contrails on radiative forcing at least partly cancels the effect of increased contrail cover. Second, our absolute radiative forcing values (which were determined using the MARQUART et al., 2003 method) are generally lower than those assumed by MARQUART et al. (2001), who relied on the respective radiative forcing estimate of the IPCC (1999) report. Hence it appears that the importance of (line-shaped) contrails as a crucial component to increase the total aircraft climate impact in case of a technology switch to cryoplanes was certainly overestimated by MARQUART et al. (2001).

Finally, we would like to note that in this paper we restricted ourselves to the contribution of line–shaped contrails. The purpose of this paper was not a complete assessment of all the possible contributions to cryoplane radiative forcing. We did not, for example, include recent investigations regarding the direct radiative forcing of aircraft water vapour emissions (GAUSS et al., 2003; MORRIS et al., 2003), or the possible climate impact of aged contrails (MANNSTEIN and SCHUMANN, 2005; MINNIS et al., 2004). Hence, this study is just forming one basic issue for a more comprehensive assessment paper, which should also include more realistic scenarios regarding the transition from conventional aviation to cryoplane air traffic.

Acknowledgements

Part of this work was funded by the EU project CRYOPLANE under grant G4RD-CT-2000-00192.

References

APPLEMAN, H., 1953: The formation of exhaust condensation trails by jet aircraft. – Bull. Amer. Meteor. Soc. **34**, 14–20.

BAUGHCUM, S.L., D.J. SUTKUS, S.C. HENDERSON, 1998: Year 2015 aircraft emission scenario for scheduled air traffic. – Tech. Rep. CR-1998-207638, NASA Langley Research Center, Hampton, VA, 44 pp.

CAEP/4-FESG, 1998: Report of the Forecasting and Economic Analysis Group: Long-Range Scenarios. – Report 4 of the International Civil Aviation Organisation (ICAO) Committee on Aviation Environmental Protection Steering Group Meeting, Canberra, Australia, 131 pp.

CHEN, J.P., 1999: Particle nucleation by recondensation in combustion exhausts. – Geophys. Res. Lett. **15**, 2403–2406.

CORCHERO, G., J.L. MONTANES, 2003: An approach to the use of hydrogen in actual commercial aircraft engines – In: Proceedings of the 16^{th} International Symposium on Air Breathing Engines (ISABE), Cleveland, Ohio, AIAA–paper 2003–1187, 8 pp.

GAUSS, M., I.S.A. ISAKSEN, S. WONG, W.-C. WANG, 2003: The impact of H_2O emissions from cryoplanes and kerosene aircraft on the atmosphere. – J. Geophys. Res. **108**, 4304, DOI: 10.1029/2002JD002623.

GIERENS, K., 1996: Numerical simulations of persistent contrails. – J. Atmos. Sci. **53**, 3333–3348.

GIERENS, K., E. JENSEN, 1998: A numerical study of the contrail-to-cirrus transition. – Geophys. Res. Lett. **25**, 4341–4344.

GIERENS, K., J. STRÖM, 1998: A numerical study of aircraft wake induced ice cloud formation. – J. Atmos. Sci. **55**, 3253–3263.

GIERENS, K., R. SAUSEN, U. SCHUMANN, 1999: A diagnostic study of the global distribution of contrails, Part II: future air traffic scenarios. – Theor. Appl. Climatol. **63**, 1–9.

HANSEN, J., M. SATO, R. RUEDY, 1997: Radiative forcing and climate response. – J. Geophys. Res. **102**, 6831–6864.

HEYMSFIELD, A.J., 1977: Precipitation development in stratiform clouds. A microphysical and dynamical study. – J. Atmos. Sci. **34**, 367–381.

IPCC, 1999: Aviation and the global atmosphere – A special report of IPCC working groups I and III. PENNER, J.E., D.H. LISTER, D.J. GRIGGS, D.J. DOKKEN, M. MCFARLAND (Eds.). Intergovernmental Panel on Climate Change. – Cambridge University Press, Cambridge, UK, 365 pp.

JÄGER, H., V. FREUDENTHALER, F. HOMBURG, 1998: Remote sensing of optical depth of aerosols and cloud cover related to air traffic. – Atmos. Environ. **32**, 3123–3127.

JENSEN, E., O.B. TOON, S. KINNE, G.W. SACHSE, B. ANDERSON, K.R. CHAN, C. TWOHY, B. GANDRUD, A. HEYMSFIELD, R.C. MIAKE-LYE, 1998: Environmental conditions required for contrail formation and persistence. – J. Geophys. Res. **103**, 3929–3936.

LAND, C., M. PONATER, R. SAUSEN, E. ROECKNER, 1999: The ECHAM4.L39(DLR) atmosphere GCM: Technical description and model climatology. – DLR-Forschungsbericht 1991-31, ISSN 1434–8454, Deutsches Zentrum für Luft- und Raumfahrt e.V. (DLR), Köln, Germany, 45 pp.

LAND, C., J. FEICHTER, R. SAUSEN, 2002: Impact of the vertical resolution on the transport of passive tracers in the ECHAM4 model. – Tellus (B) **54**, 344–360.

LEWIS, J.S., R.W. NIEDZWIECKI, 1999: Aircraft technology and its relation to emissions. – In: PENNER, J.E., D.H. LISTER, D.J. GRIGGS, D.J. DOKKEN, M. MCFARLAND (Eds.): Aviation and the global atmosphere. – IPCC, Cambridge University Press, Cambridge, UK, 217–270.

MANNSTEIN, H., U. SCHUMANN, 2005: aircraft induced contrail cirrus over Europe. – Meteorol. Z. **14**, 549–554.

MARQUART, S., B. MAYER, 2002: Towards a reliable GCM estimation of contrail radiative forcing. – Geophys. Res. Lett. **29**, 1179, DOI:10.1029/2001GL014075.

MARQUART, S., R. SAUSEN, M. PONATER, V. GREWE, 2001: Estimate of the climate impact of cryoplanes. – Aerosp. Sci. Technol. **5**, 73–84.

MARQUART, S., M. PONATER, F. MAGER, R. SAUSEN, 2003: Future development of contrail cover, optical depth and radiative forcing: Impacts of increasing air traffic and climate change. – J. Climate **16**, 2890–2904.

MCFARLANE, N.A., G.J. BOER, J.-P. BLANCHET, M. LAZARE, 1992: The Canadian Climate Centre second-generation circulation model and its equilibrium climate. – J. Climate **5**, 1013–1044.

MCFARQUHAR, G.M., A.J. HEYMSFIELD, 1998: The definition and significance of an effective radius for ice clouds. – J. Atmos. Sci. **55**, 2039–2052.

MEERKÖTTER, R., U. SCHUMANN, D.R. DOELLING, P. MINNIS, T. NAKAJIMA, Y. TSUSHIMA, 1999: Radiative forcing by contrails. – Ann. Geophysicae **17**, 1080–1094.

MINNIS, P., U. SCHUMANN, D.R. DOELLING, K. GIERENS, D.W. FAHEY, 1999: Global distribution of contrail radiative forcing. – Geophys. Res. Lett. **26**, 1853–1856.

MINNIS, P., J. K. AYERS, R. PALIKONDA, D. PHAN, 2004: Contrails, cirrus trends, and climate. – J. Climate **17**, 1671–1685.

MITCHELL, D.L., 2002: Effective diameter in radiation transfer: General definition, applications, and limitations. – J. Atmos. Sci. **59**, 2330–2346.

MORRIS, G.A., J.E. ROSENFIELD, M.R. SCHOEBERL, C.H. JACKMAN, 2003: Potential impact of subsonic and supersonic aircraft exhaust on water vapour in the lower stratosphere assessed via a trajectory model. – J. Geophys. Res. **108**, 4103, DOI:10.1029/2002JD002614.

PONATER, M., S. MARQUART, R. SAUSEN, 2002: Contrails in a comprehensive global climate model: parameterization and radiative forcing results. – J. Geophys. Res. **107**, 4164, DOI:10.1029/2001JD000429.

RÄISÄNEN, P., 1998: Effective longwave cloud fraction and maximum–random overlap of clouds: A problem and a solution. – Mon. Wea. Rev. **126**, 3336–3340.

ROECKNER, E., 1995: Parameterization of cloud properties in the ECHAM4 model. – In: Proceedings of the workshop "Cloud microphysics parameterizations in global circulation models", Kananaskis, Canada, WCRP **90**, 105–116.

ROECKNER, E., K. ARPE, L. BENGTSSON, M. CHRISTOPH, M. CLAUSSEN, L. DÜMENIL, M. ESCH, M. GIORGETTA, U. SCHLESE, U. SCHULZWEIDA, 1996: The atmospheric general circulation model ECHAM-4: Model description and simulation of present-day climate. – Report No. **218**, ISSN 0937-1060, Max-Planck-Institut für Meteorologie, Hamburg, Germany, 90 pp.

SCHMIDT, E., 1941: Die Entstehung von Eisnebel aus den Auspuffgasen von Flugmotoren. – Schriften der deutschen Akademie der Luftfahrtforschung **44**, 1–15, R. Oldenbourg, München und Berlin, Germany.

SCHMITT, A., B. BRUNNER, 1997: Emissions from aviation and their development over time. – In: SCHUMANN,

U. et al. (Eds.): Pollutants from Air Traffic – Results of Atmospheric Research 1992–1997, DLR-Mitteilungen 97–04, 37–53. – Deutsches Zentrum für Luft- und Raumfahrt e.V. (DLR), Köln, Germany.

SCHRÖDER, F., B. KÄRCHER, C. DUROURE, J. STRÖM, A. PETZOLD, J.-F. GAYET, B. STRAUSS, P. WENDLING, S. BORRMANN, 2000: On the transition of contrails into cirrus clouds. – J. Atmos. Sci. **57**, 464–480.

SCHUMANN, U., 1996: On conditions for contrail formation from aircraft exhausts. – Meteorol. Z., N.F. **5**, 4–23.

—, 2000: Influence of propulsion efficiency on contrail formation. – Aerosp. Sci. Technol. **4**, 391–401.

SCHUMANN, U., T. HAUF, H. HÖLLER, H. SCHMIDT, H. VOLKERT, 1987: A mesoscale model for simulation of turbulence, clouds and flow over mountains: Formulation and validation examples. – Beitr. Phys. Atmos. **60**, 413–446.

STRAUSS, B., R. MEERKÖTTER, B. WISSINGER, P. WENDLING, M. HESS, 1997: On the regional climatic impact of contrails: microphysical and radiative properties of contrails and natural cirrus cloud. – Ann. Geophysicae **15**, 1457–1467.

STRÖM, L., K. GIERENS, 2002: First simulations of cryoplane contrails. – J. Geophys. Res. **107**, 4346, DOI:10.1029/2001JD000838.

STUBER, N., R. SAUSEN, M. PONATER, 2001: Stratosphere adjusted radiative forcing calculations in a comprehensive climate model. – Theor. Appl. Climatol. **68**, 125–135.

SUSSMANN, R., K. GIERENS, 2001: Differences in early contrail evolution of two-engine versus four-engine aircraft: Lidar measurements and numerical simulations. – J. Geophys. Res. **106**, 4899–4911.

SVENSSON, F., A. HASSELROT, J. MOLDANOVA, 2004: Reduced environmental impact by lowered cruise altitude for liquid hydrogen–fuelled aircraft. – Aerosp. Sci. Technol. **8**, 307–320.

WYSER, K., 1998: The effective radius in ice clouds. – J. Climate **11**, 1793–1802.